IET Journals
The Institution of Engineering and Technology

Performance Evaluation of Heterogeneous Wireless Information and Power Networks

ISSN 1751-8644
doi: 0000000000
www.ietdl.org

Rui Li,[1], *Ning Cao*[1*], *Yunfei Chen*[2], *Minghe Mao*[1],

[1] *Department of Computer and Information, Hohai University, China 210098*
[2] *School of Engineering, Warwick University, UK CV4 7AL*
** E-mail: caoning@vip.163.com*

Abstract: In this paper, the performance of downlink simultaneous wireless information and power transfer (SWIPT) networks over Nakagami-m fading is analyzed. The SWIPT network is modeled as a two-tier heterogeneous network, where one tier is the information transmission network and the other is the power transmission network. The seamless integration enables both data and energy to be transferred from access points (APs) to the users. Using the stochastic geometry theory, the expressions for outage probability at the information receiver are derived in decoupled and integrated SWIPT networks. Also the average harvested energy at the power receiver is derived assuming a non-linear energy harvesting model. Simulation results validate the analytical expressions and the impact of various system parameters on the SWITP performance are investigated.

1 Introduction

1.1 Motivation and related work

Because the radio frequency (RF) can carry both information and energy, simultaneous wireless information and power transfer (SWIPT) has emerged as one of the most important technique for the fifth generation (5G) cellular networks [1]. Compared with conventional power sources, wireless power transfer provides a potentially controllable and sustainable source for wireless devices [2, 3]. Due to this, integrating wireless power transfer into conventional cellular networks has attracted much attention. This integration can be modeled as a two-tier SWIPT heterogeneous network where one tier is the information network and the other is the power network, to enable the wireless devices in the network to decode information as well as harvest energy from the RF signal. In [4], power beacons were deployed in the information networks, where the power network and information network used separate spectrum resources. In [5], an uplink cellular network overlaid with power beacons for powering mobiles. Integrated and decoupled SWIPT are currently two main architectures for the downlink SWIPT heterogeneous network, in which both energy and data are transferred from access points (APs) to user [6]-[8]. In an integrated SWIPT network, APs simultaneously transmit information and power, and receivers use the power splitter to split part of the received power for decoding and the other part for harvesting, with no requirements of deploying additional infrastructure in this scheme. For the decoupled SWIPT, some APs are assigned for information delivery (named as information access points, IAPs) and other APs are assigned for power transfer (named as energy access points, EAPs). These APs have primary differences in signal, density and transmit power due to different requirements on information and power transfer.

To further improve the area spectral efficiency, the co-existence of the information transmission networks and power transmission networks requires the sharing of the common spectrum. It is critical to accurately model and manage intra-tier and inter-tier interference received at the terminal within the network. Reference [6] analyzed the mutual interference in a planar heterogeneous network where only the strongest interference was considered. Reference [7] investigated the effect of the co-channel interference generated by wireless power transfer on the information network, provided that the number of the IAPs and EAPs were fixed. Considering the spatial distribution randomness of the APs, the coordination between the information and energy tier was conducted in [8] by using the stochastic geometry approach. References [9] and [10] investigated the performance metrics in an ad hoc network where the closed-form equations were derived for several special cases, e.g. the path loss exponent of 4 and fixed transmission-receiver separation distance. Reference [11] formulated a closed-form bound for the coverage probability in conventional cellular networks.

On the other hand, in the wireless channel, the small-scale multipath fading is commonly modeled as Rayleigh, Rician or Nakagami. A relaying cooperative communication system with SWIPT was studied in [12] over correlated Rayleigh fading channels. Reference [13] studied the device-to-device communication networks and showed that the Nakagami-m fading model provides a good fit for small scale propagation. References [14] and [15] studied the femtocell and radar heterogeneous networks with the Nakagami-m fading model, respectively. In [16], a closed-form approximation expression was provided for the coverage probability and average rate over Nakagami-m fading in multi-tier heterogeneous cellular networks. Previous works mainly focused on the performances of conventional cellular networks dedicated to information transmission over the Nakagami-m fading. The performance of the two-tier SWIPT heterogeneous network over Nakagami-m fading has not yet been derived in the literature.

These previous works have revealed that co-channel interference may have a severe adverse effect on information decoding, but it can be harvested at the device for wireless energy transfer. In [17], information delivery performance as well as energy harvesting (EH) performance were investigated using an ideal EH model. In this ideal model, the energy harvested at the end of EH circuity approximately increases linearly with the input power to the harvester. Reference [18] demonstrated that the output power is considered to be a linear function of the input power, only when the input power is very low. A more practical non-linear model has been proposed in [19] and [20] under the perfect channel state information. The non-linear characteristics reflect the actual EH performance of the SWIPT system while the non-linear EH model is more complex than the linear one. Thus the use of a suitable non-linear EH model is crucial for the accurate analysis of the SWIPT systems.

Contributions and Organization Based on the above observations, in this paper, we investigate the performance of a two-tier downlink SWIPT heterogeneous network considering both integrated and decoupled SWIPT model using the practical non-linear EH model. The APs, transmitting either data or both energy, are independently distributed following a homogeneous Poisson point process (PPP) using a common spectrum band. The information user in this area receives the desired signal from the serving AP while being

Table 1 List of Notations

Notation	Definition
Φ, λ	PPP distributed APs with density λ
P_I, P_E	Transmit power of IAP and EAP
g, m, α	Channel fading power gain, Nakagami-m fading parameter and path-loss exponent
M, s_k	M-ary QAM modulation and k-th QAM symbol
IN	Interference received at the typical receiver
SIR	Signal-to-interference-ratio
a, b, c, d	Parameters of the non-linear energy harvester circuit
$f_x(x)$	Probability density function (PDF) of x
$\mathscr{L}_x(s)$	The laplace transform of $f_x(x)$ with $\mathscr{L}_x(s) = \mathbb{E}[e^{-sx}]$
$\binom{m}{n}$	The binomial coefficient and equals to $\frac{m!}{n!(m-n)!}$
P_o^I, P_o^D	Outage probability of the integrated and decoupled SWIPT networks
${}_2F_1[.,.;.;.]$	Gauss hypergeometric function
$\gamma(\cdot,\cdot)$	Lower incomplete gamma function
$\Gamma(\cdot)$	Gamma function
E_I, E_D	Average harvested energy of the integrated and decoupled SWIPT networks

interfered by the co-channel APs. The outage probability at the information receiver and the average harvested energy at the energy receiver are derived. To the best of our knowledge, the performance analysis of the two-tier SWIPT network over the Nakagami-m fading under the non-linear EH model has not been investigated in the literature. The main contributions of this paper are as follows:

- Performance analysis for integrated and decoupled SWIPT systems are studied. Outage probability at an arbitrary information receiving node is derived over a Nakagami-m fading channel.
- An exponential function as an alternative non-linear EH model is proposed for modeling the power conversion efficiency. Then, we analytically obtain the average energy harvested at the energy receiver for both integrated and decoupled SWIPT models.
- Our numerical results compare the performances of the integrated and decoupled SWIPT models. The approximation of the outage probability provides a tight bound. For the non-linear EH model, the proposed exponential model provides a good match for the measurement data. The impacts of key system parameters are observed. We also unveil that there is a tradeoff between the outage and the harvested energy. It provides an important and useful insight on the design of the two-tier SWIPT network by quantifying the effect of intra and inter tier interference using analytical expressions and choosing the optimal parameters setting and network architecture.

Some frequently used notations in this paper are summarized in Table I. The remainder of this work is organized as follows. In Section II, the two-tier SWIPT heterogeneous system model is described. In Section III, the outage probability at a typical information receiver and average harvested energy at a typical power receiver are derived, receptively and an upper bound for outage probability is achieved. In Section IV, simulation results are shown to verify the analytical results. Finally, Section V concludes this paper.

2 System Model

We consider a two-tier downlink SWIPT heterogeneous network where the wireless information network coexists with the wireless power transfer network as depicted in Fig. 1. The receiver decodes the incoming data and/or harvest RF energy transferred from its serving AP as well as receives the interference emitted from ambient APs in this area. The APs are randomly located in the network following independent homogeneous PPPs with density λ nodes/meter^2. For simplicity, we assume that each AP serves one information/power

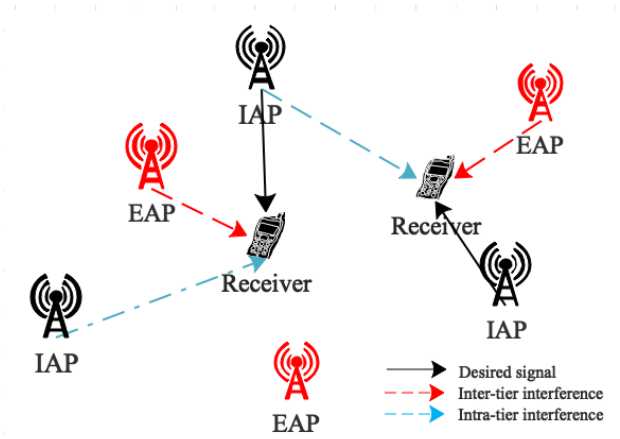

Fig. 1: The framework of a two-tier wireless SWIPT heterogeneous network.

receiver at a time. The desired and interfering channels both experience Nakagami-m fading. M-ary QAM modulation is considered at the transmitter. The k-th QAM data symbol is denoted as s_k, $k = \{1, 2, \cdots, M\}$, each with an equal probability of $p_k = 1/M$. According to Slivnyak's theorem [21], the network performance can be presented by an arbitrary receiver. Thus we investigate a typical information receiver located at the origin and the signal received at the receiver when it is associated with the nearest AP is given as:

$$y_k = \sqrt{\frac{P_I}{r_0^\alpha}} h s_k + z_0 + n_0, \quad k = 1, 2, \cdots, M, \tag{1}$$

where y_k is the corresponding received signal, P_I is the transmit power of the serving IAP, h is the channel gain between the receiver and the serving AP, which is assumed to be Nakagami-m distribution. α is the path loss exponent with $\alpha > 2$, z_0 is the interfering RF signal radiated by other APs and n_0 is the additive thermal noise, respectively, r_0 is denoted as the distance between the receiver and the serving AP. The PDF of the distance from the receiver to the nearest AP is given as

$$f_{r_0}(r) = 2\pi\lambda r \exp(-\pi\lambda r^2), \quad 0 < r < +\infty. \tag{2}$$

Considering an interference-limited heterogeneous network, the additive thermal noise could be ignored in the following analysis for simplicity. The instantaneous received SIR at the typical information receiver for the k-th sample is then expressed as

$$SIR(x) = \frac{P_I g x_k r_0^{-\alpha}}{IN}, \quad k = 1, 2, \cdots, M, \tag{3}$$

where $g = |h|^2$ is the fading power following a gamma distribution, IN is the power of the aggregate interference, x_k is the symbol energy for the k-th constellation point and is given as [22]:

$$\begin{aligned} x_k = &\frac{3}{2(M-1)}((2\lceil|k - \frac{M+1}{2}|\rceil - 1)^2 \\ &+ (2\lceil|(k \bmod \sqrt{M}) - \frac{\sqrt{M}+1}{2}|\rceil - 1)^2), \end{aligned} \tag{4}$$

where $\lceil\cdot\rceil$ is the ceiling function. $A \bmod B$ is the modular operation where A mod B equals A, if A is an integer multiple of B, or it equals to A modulo B, otherwise. The average power of the k constellation points is normalized as $\sum_{k=1}^{M} x_k/M = 1$.

In this two-tier network, the frequency resource is shared between the information and power transmission network. For the information receiver, all the APs act as the interferers except the serving AP. The interference received at the receiver is composed of the

intra-tier interference from the information network as well as the inter-tier interference from the power network. Next, we present the form of aggregate interference for integrated and decoupled SWIPT architectures, separately, which will be used in the following analysis.

Firstly, in an integrated SWIPT architecture, co-located EAPs and IAPs can transmit information and energy simultaneously. The receiver separates the received the aggregate signal power into two parts with a power splitter. For simplicity, we assume P_I is the fraction of power separated for information decoding and P_E is the other part separated for EH. All the receiving nodes decode the information signal while receiving interference from other APs except the associated AP. Thus, the aggregate interference power received from the interferes at the typical information receiver is expressed as

$$IN = \sum_{i \in \Phi \setminus \{r_0\}} (P_I + P_E) g_i r_i^{-\alpha}, \tag{5}$$

where g_i is the interfering channel fading power following the gamma distribution, r_i is the distance between the typical information receiver and the i-th interfering AP. Note that, in this scheme, the power splitting factor equals to $\frac{P_I}{P_I+P_E}$, where $P_I + P_E$ is the total transmit power required at the AP.

Secondly, in a decoupled SWIPT network, IAPs and EAPs are spatially separated where some of the APs transmit information and other APs transmit energy. We assume that each AP is individually selected to operate in information transfer mode or power transfer mode with the probability ρ at a given moment. The set of APs can then be divided into two disjoint subsets: the set of IAPs Φ_I and the set of EAPs Φ_E, such that $\Phi = \Phi_I \cup \Phi_E$. Φ_I and Φ_E can be equivalently regarded as an independent PPP where the densities of IAPs and EAPs are given as $\lambda_I = \rho\lambda$ and $\lambda_E = (1-\rho)\lambda$, respectively, following the thinning property [23]. Thus, the interference power received at the information receiver contains two parts and is given as

$$\begin{aligned} IN &= IN_I + IN_E \\ &= \sum_{i \in \Phi_I \setminus \{r_0\}} P_I g_i r_i^{-\alpha} + \sum_{i \in \Phi_E} P_E g_i r_i^{-\alpha}, \end{aligned} \tag{6}$$

where P_I and P_E denotes the transmit power of IAP and EAP, respectively. Specially, the first term in (6) represents the intra-tier interference from the IAPs within Φ_I and the second term in (6) represents the inter-tier interference from the EAPs within Φ_E.

3 Performance Evaluation

In this section, we first derive the outage probability at the typical information receiver and a closed-form bound on the outage probability by using the Alzer's inequality. Then we obtain the average received power at the typical energy receiver under the non-linear model.

3.1 Outage probability at the typical information receiver

For the information receiver, an outage can occur when the SIR is below a predefined threshold which is defined as

$$\begin{aligned} P_o &= Pr(SIR(x) < \theta) \\ &= \frac{1}{M} \sum_{k=1}^{M} Pr(SIR(x) < \theta | x = x_k), \end{aligned} \tag{7}$$

where θ is the information reception threshold. Note that, the outage probability P_o needs to be averaged with respect to the distance, channel fading and spatial nodes distribution due to the inherent randomness of the network. Specifically, the conditional outage probability for x_k is expressed as

$$\begin{aligned} &Pr(SIR(x) < \theta | x = x_k) \\ &= 1 - Pr(\frac{P_I g x_k r_0^{-\alpha}}{IN} \geq \theta) \\ &= 1 - \int_0^{+\infty} Pr(\frac{P_I g x_k r^{-\alpha}}{\theta} \geq IN | r) f_{r_0}(r) dr, \end{aligned} \tag{8}$$

where

$$\begin{aligned} &Pr(\frac{P_I g x_k r^{-\alpha}}{\theta} \geq IN | r) \overset{(a)}{=} \\ &\qquad \int_{-\infty}^{+\infty} \mathscr{L}_{IN|r_0}(2\pi i s) \frac{\mathscr{L}_{g|r_0}(-2\pi i s \zeta) - 1}{2\pi i s} ds, \end{aligned} \tag{9}$$

with $\zeta = \frac{P x_k}{\theta r^{\alpha}}$. In (9), equation (a) is achieved by using Plancheral-Parseval theorem [24]. $\mathscr{L}_{g|r_0}(s)$ is the conditional Laplace transform of the channel fading power g given r_0 and given as $\mathscr{L}_{g|r_0}(s) = (1+s)^{-m}$ for Nakagami-m fading, where m is an integer. $\mathscr{L}_{IN|r_0}(s)$ is the conditional Laplace transform of the aggregate interference IN when r_0 is given.

The conditional Laplace function of interference power can be derived using Moment Generating Function (MGF) over the interference, i.e., $\mathscr{L}_{IN|r_0}(s) = \mathbb{E}_{IN|r_0}[e^{-sIN}]$ for the integrated SWIPT. For the decoupled SWIPT architecture, the conditional Laplace function could be written in terms of the Laplace transform of intra- and inter-tier interference and is given as

$$\begin{aligned} \mathscr{L}_{IN|r_0}(s) &= \mathbb{E}[\exp(-s(IN_I + IN_E))] \\ &= \mathbb{E}[\exp(-sIN_I)]\mathbb{E}[\exp(-sIN_E)] \\ &= \mathscr{L}_{IN_I|r_0}(s)\mathscr{L}_{IN_E|r_0}(s). \end{aligned} \tag{10}$$

The conditional Laplace transform $\mathscr{L}_{IN_I|r_0}$ and $\mathscr{L}_{IN_E|r_0}$ follow an identical distribution. Furthermore, the Laplace function of each tier $\mathscr{L}_{IN_l|r_0}$ is given by

$$\begin{aligned} &\mathscr{L}_{IN_l|r_0}(s) \\ &= \mathbb{E}_{\Phi_l}[\exp(-s \sum_{i \in \Phi_l} P_l g_i r_i^{-\alpha})] \\ &\overset{(a)}{=} \mathbb{E}_g[\exp(-\lambda_l \int_{\mathbb{R}^2} 1 - e^{-sP_l g_i r^{-\alpha}} dr)] \\ &\overset{(b)}{=} \exp(-2\pi\lambda_l \int_{r_0}^{+\infty} (1 - \mathbb{E}_g[e^{-sP_l g_i r^{-\alpha}}]) r dr) \\ &\overset{(c)}{=} \exp(-2\pi\lambda_l \int_{r_0}^{+\infty} (1 - \frac{1}{(1+sP_l r^{-\alpha})^m}) r dr) \\ &\overset{(d)}{=} \exp(-\pi\lambda_l r_0^2 ({}_2F_1[m, -\frac{2}{\alpha}; -\frac{2}{\alpha}+1; -\frac{sP_l}{r_0^{\alpha}}] - 1)), \end{aligned} \tag{11}$$

where $l \in \{I, E\}$ corresponds to the information tier and power tier, λ_l is the density of the IAP/EAP. (a) and (b) follow with the Campbell theorem for PPP and the Jensen's inequality, respectively, (c) follows the MGF of gamma distribution, and (d) follows [25, eq. (5)]. Substituting (8)-(11) in (7), the outage probability P_o^I for integrated SWIPT could be given by (12) as shown at the top of this page, where $G(x) = ((1-\zeta x)^{-m} - 1)/x$. Similarly, the outage probability P_o^E for the decoupled SWIPT is expressed as is derived in (13) as shown at the top of this page.

The exact expressions in (12) and (13) are general enough for different path loss and fading parameters. However, the results in two-fold integral forms are not closed-form and cause difficulty in computation and analysis. On further simplification, a closed-form approximate expression of the outage probability is derived by using stochastic geometry approach to solve the resulting integrals. The

$$P_o^I = 1 - \frac{1}{M}\sum_{k=1}^{M}\int_{-\infty}^{+\infty}\int_{0}^{+\infty} 2\pi\lambda r \cdot G(2\pi i s)\cdot e^{-\pi\lambda r_0^2 {}_2F_1[m,-\frac{2}{\alpha};-\frac{2}{\alpha}+1;-\frac{2\pi i s P_I}{m r^{\alpha}}]} dr ds. \quad (12)$$

$$P_o^D = 1 - \frac{1}{M}\sum_{k=1}^{M}\int_{-\infty}^{+\infty}\int_{0}^{+\infty} 2\pi\lambda r \cdot G(2\pi i s)\cdot e^{-\pi\lambda\rho r_0^2 {}_2F_1[m,-\frac{2}{\alpha};-\frac{2}{\alpha}+1;-\frac{2\pi i s P_I}{m r^{\alpha}}]-\pi\lambda r_0^2(1-\rho){}_2F_1[m,-\frac{2}{\alpha};-\frac{2}{\alpha}+1;-\frac{2\pi i s P_E}{m r^{\alpha}}]} dr ds. \quad (13)$$

average outage probability of the integrated SWIPT system is given as

$$\begin{aligned}
P_o^I &= \frac{1}{M}\sum_{k=1}^{M} Pr(SIR(x) < \theta | x = x_k) \\
&= \frac{1}{M}\sum_{k=1}^{M}\int_0^{+\infty} Pr(\frac{P_I g x_k r^{-\alpha}}{IN} < \theta | r) f_{r_0}(r) dr \\
&= \frac{1}{M}\sum_{k=1}^{M}\int_0^{+\infty} 2\pi\lambda r e^{-\pi\lambda r^2}\mathbb{E}_{IN}[Pr(g < \frac{\theta IN}{P_I x_k r^{-\alpha}} | r, IN)] dr \\
&= \frac{1}{M}\sum_{k=1}^{M}\int_0^{+\infty} 2\pi\lambda r e^{-\pi\lambda r^2}\mathbb{E}_{IN}[\frac{\gamma(m, \frac{\theta IN}{P_I x_k r^{-\alpha}})}{\Gamma(m)} | r] dr.
\end{aligned} \quad (14)$$

According to the Alzer's inequality [26], an upper bound for $\gamma(m,x)/\Gamma(m)$ is given as

$$\frac{\gamma(m,x)}{\Gamma(m)} \leq (1 - e^{-\frac{x}{(\Gamma(m+1))^{1/m}}})^m, \quad x > 0 \quad (15)$$

where the equality holds when $m = 1$. Following (15), the conditional outage probability can be expanded as

$$\begin{aligned}
&\mathbb{E}_{IN}[\frac{\gamma(m, \frac{\theta IN}{P_I x_k r^{-\alpha}})}{\Gamma(m)} | r] \\
&\leq \int_0^{+\infty} (1 - e^{-s\eta r^{\alpha}})^m f_{IN}(s) ds \\
&\overset{(a)}{=} \sum_{n=0}^{m}(-1)^n \binom{m}{n} \int_0^{+\infty} e^{-sn\eta r^{\alpha}} f_{IN}(s) ds \\
&\overset{(b)}{=} \sum_{n=0}^{m}(-1)^n \binom{m}{n} \mathscr{L}_{IN|r_0}(n\eta r^{\alpha}) \\
&= \sum_{n=0}^{m}(-1)^n \binom{m}{n} e^{-\pi\lambda r^2({}_2F_1[m,-\frac{2}{\alpha};\frac{\alpha-2}{\alpha};-n\eta P_l]-1)},
\end{aligned} \quad (16)$$

where $\eta = \frac{\theta}{P_I x_k (\Gamma(m+1))^{1/m}}$, $f_{IN}(\cdot)$ is the PDF of interference, step (a) follows from the binomial theorem, step (b) follows from the definition of Laplace transform. By substituting (11) into (16) and taking the expectation over the transmitter-receiver distance, the closed-form expression for the outage probability in the integrated SWIPT architecture is then given as

$$\begin{aligned}
P_o^I &= \frac{1}{M}\sum_{k=1}^{M}\int_0^{+\infty} 2\pi\lambda r e^{-\pi\lambda r^2}\mathbb{E}_{IN}[\frac{\gamma(m, \frac{\theta r^{\alpha} IN}{P_I x_k})}{\Gamma(m)} | r] dr, \\
&\leq \frac{1}{M}\sum_{k=1}^{M}\sum_{n=0}^{m}(-1)^n \binom{m}{n} \int_0^{+\infty} 2\pi\lambda r e^{-\pi\lambda r^2 \beta(m,\alpha,P_I)} dr \\
&= \frac{1}{M}\sum_{k=1}^{M}\sum_{n=0}^{m}(-1)^n \binom{m}{n} \frac{1}{\beta(m,\alpha,P)},
\end{aligned} \quad (17)$$

where $\beta(m,\alpha,P) = {}_2F_1[m,-\frac{2}{\alpha};\frac{\alpha-2}{\alpha};-n\eta P]$ and $P = P_I + P_E$. Similarly, the closed-form bound for the decoupled SWIPT network is given as

$$\begin{aligned}
P_o^D &= \frac{1}{M}\sum_{k=1}^{M} Pr(SIR(x) < \theta | x = x_k) \\
&= \frac{1}{M}\sum_{k=1}^{M}\int_0^{+\infty} Pr(\frac{P_I g x_k r^{-\alpha}}{IN_I + IN_E} < \theta | r) f_{r_0}(r) dr \\
&= \frac{1}{M}\sum_{k=1}^{M}\int_0^{+\infty} \mathbb{E}_{IN}[\frac{\gamma(m, \frac{\theta r^{\alpha}}{P_I x_k}(IN_I + IN_E))}{\Gamma(m)} | r] f_{r_0}(r) dr, \\
&\leq \frac{1}{M}\sum_{k=1}^{M}\sum_{n=0}^{m}(-1)^n \binom{m}{n} \mathbb{E}_r[\mathscr{L}_{IN_I|r_0}(n\eta r^{\alpha})\mathscr{L}_{IN_E|r_0}(n\eta r^{\alpha})] \\
&= \frac{1}{M}\sum_{k=1}^{M}\sum_{n=0}^{m}\frac{(-1)^n\binom{m}{n}}{\rho\beta(m,\alpha,P_I) + (1-\rho)\beta(m,\alpha,P_E).}
\end{aligned} \quad (18)$$

The closed-form expressions in (17) and (18) provide an upper bound on the outage probability and reduce the computing complexity by avoiding the integral form. We can also see that the outage probability does not depend on the AP density. It means deploying more APs in the network does not affect the outage behavior, because the increased received power of the desired signal helps counteract the increased interference. Next, we present the results for the average harvester energy at the typical energy receiver.

3.2 Average harvested energy at the typical power receiver

In this paper, we assume a non-linear model for the power conversion efficiency. The model in [20] does not lead to mathematical tractability. Thus, we approximate this model using a sum of two exponential functions of the input power, as

$$E = ae^{bP_{in}} + ce^{dP_{in}}, \quad (19)$$

where P_{in} is the input power, $a, b, c, d \in \mathbb{R}$ are the parameters of the non-linear model and depended on the actual hardware EH hardware circuit of the harvester.

For the integrated SWIPT network, the energy receiver equipped with a power splitter could harvest part of energy from the received aggregate power. Furthermore, we assume that the thermal noise could be neglected because it is much smaller than the total interference power. The power input to the typical receiver is given as

$$P_{in} = \sum_{i\in\Phi} P_E g_i r_i^{-\alpha}. \quad (20)$$

The average harvested energy at the typical receiver can be derived by using the MGF of P_{in} from (11), as

$$\begin{aligned}
E_I &= \mathbb{E}[ae^{bP_{in}} + ce^{dP_{in}}] \\
&= a\mathbb{E}[e^{bP_{in}}] + c\mathbb{E}[e^{dP_{in}}] \\
&= a\mathbb{E}_{\Phi}[e^{b\sum_{i\in\Phi} P_E g_i r_i^{-\alpha}}] + c\mathbb{E}_{\Phi}[e^{d\sum_{i\in\Phi} P_E g_i r_i^{-\alpha}}] \\
&= ae^{-\pi\lambda v_0^2(\beta_0(b,P_E)-1)} + ce^{-\pi\lambda v_0^2(\beta_0(d,P_E)-1)},
\end{aligned} \quad (21)$$

where $\beta_0(b, P_E) = {}_2F_1(m, -\frac{2}{\alpha}, \frac{\alpha-2}{\alpha}, \frac{bP_E}{v_0^\alpha})$ and $v_0 \geq 1$ is a small constant to avoid singularity at zero distance [27].

In the decoupled SWIPT architecture, the interference power degrades the performance of the information receivers but could be harvested at the power receive. The received power at a typical power receiver is expressed as

$$P_{in} = \sum_{i\in\Phi_I} P_I g_i r_i^{-\alpha} + \sum_{i\in\Phi_E} P_E g_i r_i^{-\alpha}. \tag{22}$$

Then, the average harvested energy at the receiver can be expressed as

$$\begin{aligned} E_D &= \mathbb{E}[ae^{bP_{in}} + ce^{dP_{in}}] \\ &= a\mathbb{E}[e^{bP_{in}}] + c\mathbb{E}[e^{dP_{in}}] \\ &= ae^{-\pi\lambda v_0^2(\beta_1(b,P_I,P_E)-1)} + ce^{-\pi\lambda v_0^2(\beta_1(d,P_I,P_E)-1)}, \end{aligned} \tag{23}$$

where $\beta_1(b, P_I, P_E) = \rho\beta_0(b, P_E) + (1-\rho)\beta_0(b, P_I)$.

4 Numerical Results and Discussion

In this section, numerical results in terms of the outage probability and average harvested energy at the receiver are presented for the integrated SWIPT (I-S) and decoupled SWIPT (D-S) architecture. The analytical results of the outage probability are obtained from (17)-(18) with a computational complexity of $\mathcal{O}(M(m+1))$. The larger the fading parameter m is, the higher the computation complexity will be. The simulation results are obtained by the Monte Carlo simulation (averaged over 10^4 simulation runs). In the simulation, APs are distributed as independent homogeneous PPP with density λ. The typical receiver is located at the origin. Both the desired and interfering channels are experiencing the Nakagami-m fading with the shape parameter m. 16-QAM modulation is set for all cases. The parameters a, b, c, d are determined by data fitting tools using the data from [20] with $a = 0.025, b = -0.0016, c = -0.025$ and $d = -602.1$.

Fig. 2 shows the outage probability at the information receiver in terms of the SIR threshold for transmitting power P_E with I-S and D-S networks. It can be seen that the results generated using the obtained closed-form approximate expressions for the outage probability are very close to the simulation results, which corroborates our analysis. All the cures have the same trend, as the outage probability increases with the SIR threshold increases since the received SIR is less likely to achieve the threshold. As P_E increases from 36 dBm to 40 dBm, the outage probability decreases. The higher value of P_E indicates stronger interference and weaker transmission reliability for the information receiver. For the I-S architecture, the power of P_E does not affect the outage probability in the interference-limited scheme. It also shows that D-S has a lower outage probability than I-S in all cases because I-S has the largest degradation.

Fig. 3 shows the outage probability at the information receiver in terms of the information threshold and shape parameter m over Nakagami-m fading for the I-S and D-S networks. It can be observed from the plot that the outage probability increases as the value of m decreases from 4 to 2. This is because the channel experiences more serious fading for small m. The analytical results are very close to Monte Carlo results when $m = 2$. There is only a negligible error for high SNR threshold and large m. It confirms that the closed-form expression provides a reliable upper bound to the SWIPT heterogeneous network and can be extended to analyze the outage probability in any generalized fading.

Fig. 4 shows the outage probability at the information receiver in terms of the SIR threshold for path loss α in I-S and D-S networks. As shown, the outage probability decreases with increasing α in both the I-S and D-S network. It implies that the outage behavior is degraded in an urban environment (path loss exponent of 3.5) compared with the performance in a rural environment (path loss exponent of 2.5). This is because the increasing path loss leads to the

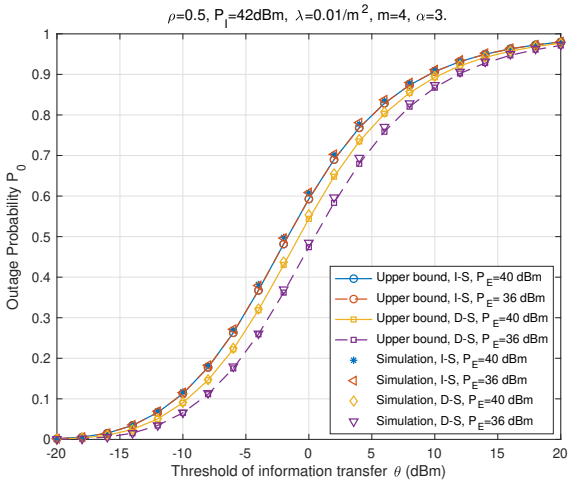

Fig. 2: Outage probability of simulation and the bound for P_E={40dBm, 36dBm} in I-S and D-S architectures.

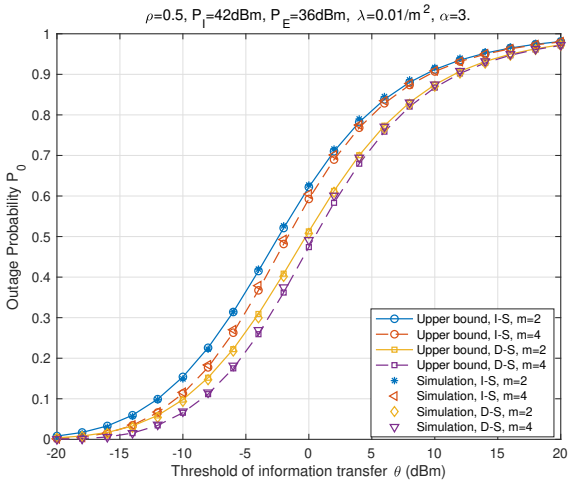

Fig. 3: Outage probability of simulation and the bound for m={2, 4} in I-S and D-S architectures.

small desired power and interference power received at the information receiver, while the path loss seems to affect more interference than desired signal. It can be seen that the outage performance hugely depends on the propagation environment.

Fig. 5 shows the effects of the node density λ and transmit power on the average harvested energy with the practical non-linear EH circuits under I-S and D-S architectures. One sees that the analytical results closely match the non-linear EH model proposed in [20]. The harvested energy increases with the density of nodes and achieves the maximum value when the input power is greater than the fixed value, regardless of receiver structures. It also shows that the average harvested energy at the typical receiver increases with the increase of the transmit power in the power transmission tier. D-S performs better than I-S at the high transmit power domain. In addition, it shows that the improvement is considerable in the I-S and minor in the D-S with respect to the transmit power P_E. Increasing transmit power in the power transfer tier improves the EH performance, in contrast to the more outage in the information receiver. There is a tradeoff between the outage probability and average harvested energy.

Fig. 6 shows the effects of the node density λ and channel fading parameter m on the average received power received at the power receiver with I-S and D-S architectures. The average received power is greatly increased when the number of APs increases because more interference is introduced in the network that can be harvested at the power receiver. For a given density, the average received power at the

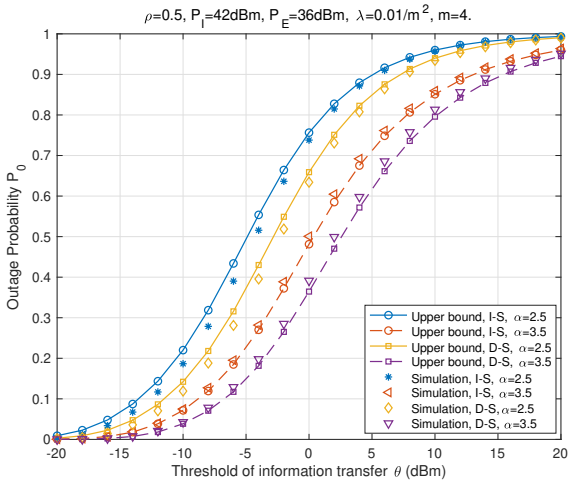

Fig. 4: Outage probability of received power of simulation and the bound for α={2.5, 3.5} in I-S and D-S architectures.

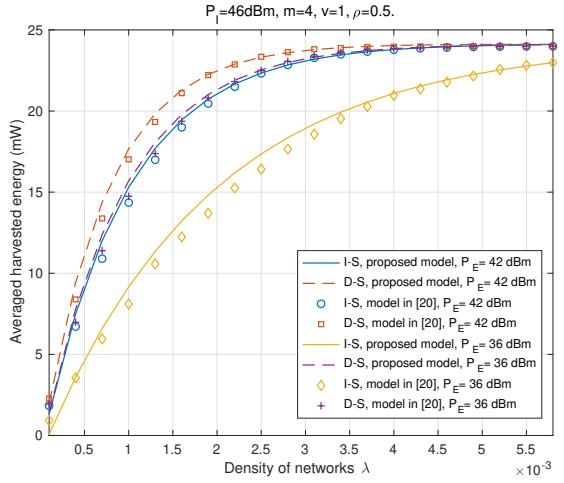

Fig. 5: Average received power of simulation and the bound for P_E={40dBm, 44dBm} in I-S and D-S architectures.

receiver increases when m increases from 2 to 4 because the lower m corresponds to severe fading. It indicates that the channel fading plays a dominant role in the performance of the power transmission tier. The D-S has a larger average received power than I-S in both cases because a fraction of received power is utilized for information decoding in I-S.

5 Conclusion

In this paper, we study the performance of a two-tier wireless downlink heterogeneous network with the integrated and decoupled SWIPT architectures. Closed-form approximate expressions for the outage probability at the information receiver have been derived over Nakagami-m fading by the stochastic geometry approach. Averaged harvested energy also has been derived under the proposed non-linear EH model. The validity has been verified by the numerical results. The analysis of the outage probability and average harvested energy provided a useful guideline on the design of the energy efficient SWIPT system by taking into account key system parameters such as the transmit power of EAP and IAP, density of networks, and fading scenarios.

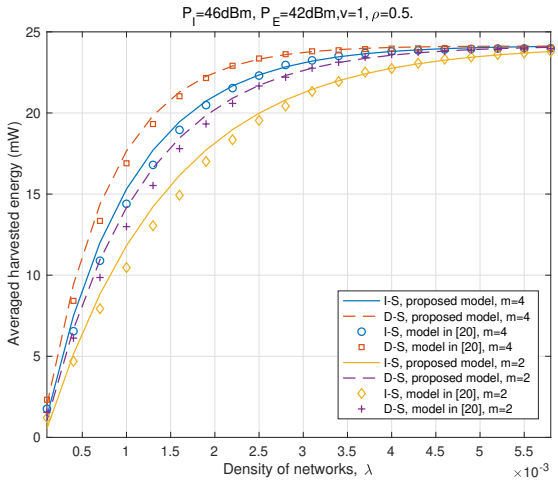

Fig. 6: Average received power of simulation and the bound for m={2, 4} in I-S and D-S architectures.

6 Acknowledgments

Rui Li is indebted to the China Scholarship Council (CSC) for its financial support as a visiting Ph.D. student at the University of Warwick. This work was partially supported in part by the National Natural Science Youth Foundation of China under Grant 61701167, and the Fundamental Research Funds for the Central Universities under Grant 2019B00814.

7 References

1 Hussein H. S., Elsayed M., Mohamed U. S.: 'Spectral efficient spatial modulation techniques', *IEEE Access*, 2019, **7**, pp. 1454–1469
2 Thangaraj C. A., Velkennedy A., Ponmani S.: 'Simultaneous wireless information and power transfer in energy-augmented amplify and forward cooperative cognitive networks', *IET Commun.*, 2016, **13**, pp. 2186–2191
3 Zhang G., Yang L., Li X., Li G., Cui M.: 'Signal and artificial noise beamforming for secure simultaneous wireless information and power transfer multiple-input multiple-output relaying systems,' *IET Commun*, 2016, **10**, pp. 796–804
4 Guo J., Durrani S., Zhou X., Yanikomeroglu H.: 'Outage Probability of Ad Hoc Networks With Wireless Information and Power Transfer,' *IEEE Wirel. Commun. Lett.*, 2015, **4**, pp. 409–412
5 Huang K and V.K.N.Lau,: 'Enabling wireless power transfer in cellular networks: architecture, modeling and deployment,' *IEEE Trans. Wireless Commun.*, 2014, **13**, pp. 902–912
6 Munari A., Simic L., Petrova M.: 'Stochastic Geometry Interference Analysis of Radar Network Performance,' *IEEE Commun. Lett.*, 2018, **22**, pp. 2362–2365
7 Chen Y., et al.: 'Interference Analysis in Wireless Power Transfer,' *IEEE Commun. Lett.*, 2017, **21**, pp. 2318–2321
8 Park J, Clerckx B, Song C, and Wu Y,: 'An Analysis of the Optimum Node Density for Simultaneous Wireless Information and Power Transfer in Ad Hoc Networks,' *IEEE Trans. Veh. Techn.*, 2017, **67**, pp. 2713–2726
9 Park J.: 'Outage probability of simultaneous wireless information and power transfer in heterogeneous information/energy ad hoc networks,' in *Int. Conf. on Elec. Inform. and Commun. (ICEIC)*, Honolulu, HI, 2018, pp. 1–4
10 Hunter A. M., Andrews J G., Weber S.: 'Transmission capacity of ad hoc networks with spatial diversity,' *IEEE Trans. on Wirel. Commun.*, 2008, **7**, pp. 5058–5071
11 Joshi S., Mallik R. K.: 'Coverage Probability Analysis in a Device-to-Device Network: Interference Functional and Laplace Transform Based Approach,' *IEEE Commun. Lett.*, 2019, **23**, pp. 466–469
12 Jin N., Yang L., Jin X., Chen D.: 'Performance Analysis of Wireless Energy Harvesting Cooperative System with Precoding Spatial Modulation,' *IET Comm.*, 2019, **13**, pp. 2369–2374
13 Joshi S., Mallik R. K., 'Analysis of dedicated and shared device-to-device communication in cellular networks over Nakagami-m fading channels', *IET Commun.*, 2017, **11**, pp. 1600–1609
14 Chen S., Jin H., Li Y., Peng M.: 'Performance analysis of two-tier femtocell networks in Nakagami-m fading channels,' *2013 Int. Conf. on Wireless Commun. and Signal Proc.*, Hangzhou, 2013, pp. 1–5
15 Khawar A., Abdelhadi A., Clancy T. C.: 'Coexistence Analysis Between Radar and Cellular System in LoS Channel,' *IEEE Antennas Wirel. Propag. Lett.*, 2016, **15**, pp. 972–975
16 Praneeth Varma G. V. S. S., Sharma G. V. V., Kumar A.: 'Closed-form Approximations for Coverage and Rate in a Multi-tier Heterogeneous Network in Nakagami-m Fading,' *2018 24th National Conf. on Commun. (NCC)*, 2018, Hyderabad, pp. 1–6
17 Liu W., Zhou X., Durrani S., and Popovski P.: 'SWIPT with practical modulation and RF energy harvesting sensitivity,' in *Proc. IEEE Int. Conf. Commun. (ICC)*,

2016, pp. 1–7
18 Yu. Z, Chi. K, adn et al:, 'Energy Provision Minimization in Wireless Powered Communication Networks With Node Throughput Requirement,' *IEEE Trans. on Veh. Techn.*, 2019, **68**, pp. 7057–7070
19 Zhou F., et al:'Artificial Noise Aided Secure Cognitive Beamforming for Cooperative MISO-NOMA Using SWIPT,' *IEEE Journal on Selected Areas in Commun*., 2018, **36**, pp. 918–931
20 X Zhang, et.al: 'Robust resource allocation for MISO cognitive radios networks under two practical non-linear energy harvesting model,' *IEEE Commun. Lett*., 2018, **22**, pp. 1874–1877
21 Haenggi M.: 'Stochastic geometry for wireless networks', New York, NY, USA: Cambridge Univ. Press, 2013
22 Liu W., Zhou X., Durrani S., Popovski P.: 'SWIPT with practical modulation and RF energy harvesting sensitivity,' in *2016 IEEE Int. Conf. on Commun. (ICC)*, Kuala Lumpur, 2016, pp. 1–7
23 Kim Y., Lee T., Kim D.: 'Joint Information and Power Transfer in SWIPT-enabled CRFID Networks,' *IEEE Wireless Commun. Lett.,* 2018, **7**, pp. 186–189
24 Andrews J. G., Baccelli F., Ganti R. K.: 'A Tractable Approach to Coverage and Rate in Cellular Networks,' *IEEE Trans. on Commun.*, 2011, **59**, pp. 3122–3134
25 S. T. Veetil, K. Kuchi, A. K. Krishnaswamy, and R. K. Ganti, 'Coverage and rate in cellular networks with multi-user spatial multiplexing,' in *2013 IEEE Int. Conf. on Commun. (ICC)*, 2013, pp. 5855–5859
26 Bai T., Heath R. W.: 'Coverage and Rate Analysis for Millimeter-Wave Cellular Networks,' *IEEE Trans. on Wirel. Commun.,* 2014, **14**, pp. 1100–1114
27 Shang B., Zhao L., Chen K., Chu X.: 'Energy Efficient D2D-Assisted Offloading with Wireless Power Transfer,' in *IEEE Global Commun. Conf*., Singapore, 2017, **19**, pp. 167–203